PAPER • OPEN ACCESS

Creep-rupture behavior of a nickel-based single crystal superalloy

To cite this article: Weiwei Liu *et al* 2019 *IOP Conf. Ser.: Mater. Sci. Eng.* **605** 012021

View the article online for updates and enhancements.

This content was downloaded from IP address 222.184.59.219 on 31/10/2019 at 09:08

Creep-rupture behavior of a nickel-based single crystal superalloy

Weiwei Liu[1,*], Yuanyuan Guo[1],Mai Zhang[1,2], Jichun Xiong[1], Jian Zhang[1]

1. Science and Technology on Advanced High Temperature Structural Materials Laboratory, Beijing Institute of Aeronautical Materials, Beijing 100095, P.R. China
2. School of Materials Science and Engineering at University of Science and Technology Beijing 100083, P.R. China)
E-mail: liuww_80@sina.com

Abstract. A first generation single crystal superalloy was employed to research the high temperature creep behavior. Scanning electron microscope (SEM), transmission electron microscope (TEM) are used. The main results are summarized below: There are two mechanisms for the steady creep. The first one is superlattice dislocation cutting γ′ precipitates, which is the main mechanism for 1000℃ creep behavior. In this case, the creep rate increases when the γ/γ′ microstructure undergoes topological inversion, which leads to a rapid increase in the density of γ′ cutting dislocation. The second mechanism is transverse climb of a/2<110> interfacial dislocation, which is the main mechanism for 1100℃ creep behavior. In this case, climb of interfacial dislocations produced most of the steady creep strain. A by-product is the vacancies diffusing along the interfaces and low angle boundary to pores.

Key words: single crystal ；superalloy ；high temperature creep ；dislocation ；porosity

Nickel-based single crystal superalloys have been widely used in the manufacturing of aero-engine turbine blades because of its excellent high temperature creep strength and fatigue strength, as well as good thermal corrosion resistance and oxidation resistance[1,2]. With the increasing temperature of the advanced aero-engine turbine, high temperature creep deformation and fracture become one of the main failure forms of single crystal turbine blades. The creep behavior of nickel-based single crystal superalloy under typical temperature stress has been widely studied [3-8], and the research mainly focuses on the microstructure

Content from this work may be used under the terms of the Creative Commons Attribution 3.0 licence. Any further distribution of this work must maintain attribution to the author(s) and the title of the work, journal citation and DOI.
Published under licence by IOP Publishing Ltd

evolution, the deformation mechanism of different creep stages and the prediction model of creep life, in which the directional coarsening of γ′ phase is a typical phenomenon in the medium and high temperature creep process of single crystal alloy. However, there is no unified conclusion about its effect on the properties of alloys. Furthermore, the creep deformation mechanism of single crystal alloy at about 760 °C has been thoroughly studied[9,10]. The research indicates that the creep behavior and deformation mechanism of single crystal superalloys are influenced by experimental temperature, stress range, loading mode and so on. This is mainly caused by the interaction between dislocations and γ′ particles. With the changes of these factors, both of the creep and deformation mechanism of the alloy are changing[11-19]. Generally, there are still few researches on creep deformation mechanism of single crystal alloys at high temperature level, i.e. 1100 °C, especially existing plenty of problems to be studied in the third stage of creep deformation and creep fracture mechanism.

In this present work, a nickel-based single crystal superalloy was employed to study the high temperature creep under low applied stress behavior at 1000 °C and 1100 °C. The high temperature creep behavior, creep deformation, fracture characteristics and mechanism of single crystal alloy were systematically studied and analyzed. The different of creep mechanisms at two temperature were also compared. Results documented in this study should be able to provide an experimental basis for the utilization of single crystal alloy under high temperature conditions, and further improve the creep theory of nickel-based single crystal superalloy.

1. Experimental materials and procedures

The experimental material was the first generation of nickel-based single crystal superalloy with chemical compositions of Ni-Cr-W-Ta-Al-Co-Ti-Mo system. The constant load tensile creep test was carried out on high temperature creep machine with applied stress ranging from 120 to 220 MPa, and the experimental temperature were 1000 °C and 1100 °C. The furnace temperature was controlled by the upper, middle and lower platinum-rhodium thermocouples which placed in the normal distance part of the specimens, and the temperature controlled within ±2 °C. creep strain was measured by an extensometer connected to the shoulders of creep specimens, the accuracy was 5×10-4~5×10-5and experimental environment was air. Most of specimens were pulled to fracture, part of specimens was subjected to creep interruption test for the observation of microstructure.

The specimens after creep fracture and interruption test were observed and analyzed by JSM-6301 field emission scanning electron microscopy and Tecnai G 20 transmission electron microscopy (TEM). When preparing TEM specimens, 0.5 mm thick sheets were cut along the direction perpendicular to the tensile axis and 5-10 mm away from the tensile fracture. Firstly, mechanically ground to below 50 μm, then double jet electrolysis was used to reduce the thickness. The electrolyte was composed of 10% perchloric acid and 90% alcohol.

2. Results and discussion

2.1. High temperature creep properties of experimental alloy

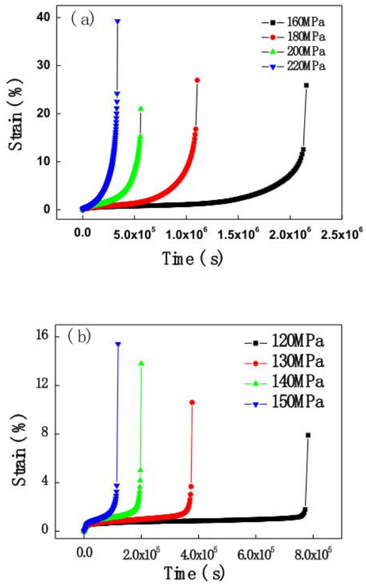

Figure 1. Typical creep curves of experimental alloy:
(a) 1000 °C and (b) 1100 °C

Figure 1 shows the typical creep curves of experimental alloy under different stress levels at 1000 °C and 1100 °C. As can be seen from the strain vs. time relationship, the main characteristics of high temperature creep behavior of experimental alloy are as follows:

(1)Both the creep curves at 1000 °C and 1100 °C exhibit three stage of creep characteristics, i.e. initial creep, steady creep and accelerated creep. The duration of creep steady-state stage at 1100 °C accounts for a higher proportion of the whole creep life, and the creep curve shows a clear platform shape.

(2)The creep extension decreases obviously when the experimental temperature increasing from 1000 °C to 1100 °C. Under the conditions of 1000 °C and 160 MPa – 220 MPa, the fracture extension ranges from 20% to 40%. Compared with the former, the extension at 1100 °C ranges from 8% to 16%, which is obviously smaller than that of the former.

(3)In the creep test at 1000 °C, the strain rate rises slowly after alloy entering the third stage of creep. While in the test at 1100 °C, the strain rate rises rapidly after the beginning of the third stage of creep, and fracture occurs in a short period of time.

2.2. Microstructural evolution of creep process

As can be seen from figure 2a and b, the shaped raft of directional coarsening of γ′ phaseoccurs during the creep test at high temperature ranging from 1000 °C to 1100 °C. The alloy belongs to negative misfit alloys, hence the raft structure perpendicular to the direction of applied stress formed under tensile stress. The dislocation configuration observed by TEM shows that complete and regular dislocation network at the γ/γ′ interface is rapidly formed during creep at 1000 °C and 1100 °C. The formation of dislocation network originates from the reaction between dislocations at the γ/γ′ interface, which generally acts as impediment for dislocation movement and reduces creep rate. figure 2c and d reveal that superlattice dislocation cutting γ′ phase occurs at both temperature in the post stage of creep, which is the main deformation mechanism of creep steady-stare stage. In contrast, the greater number of dislocations are cut into γ′ phase and show multiple morphologies under 1000 °C and higher stress condition. However, there are only few dislocations are cut under 1100 °C and higher stress condition, and mainly exist in a single form of screw dislocations. This is the biggest difference between the creep deformation mechanism at 1100°C and 1000 °C. It indicates that large number of dislocations can not be cut into γ′ phase due to insufficient applied stress, hence the dislocation configuration does not change significantly during the whole creep process.

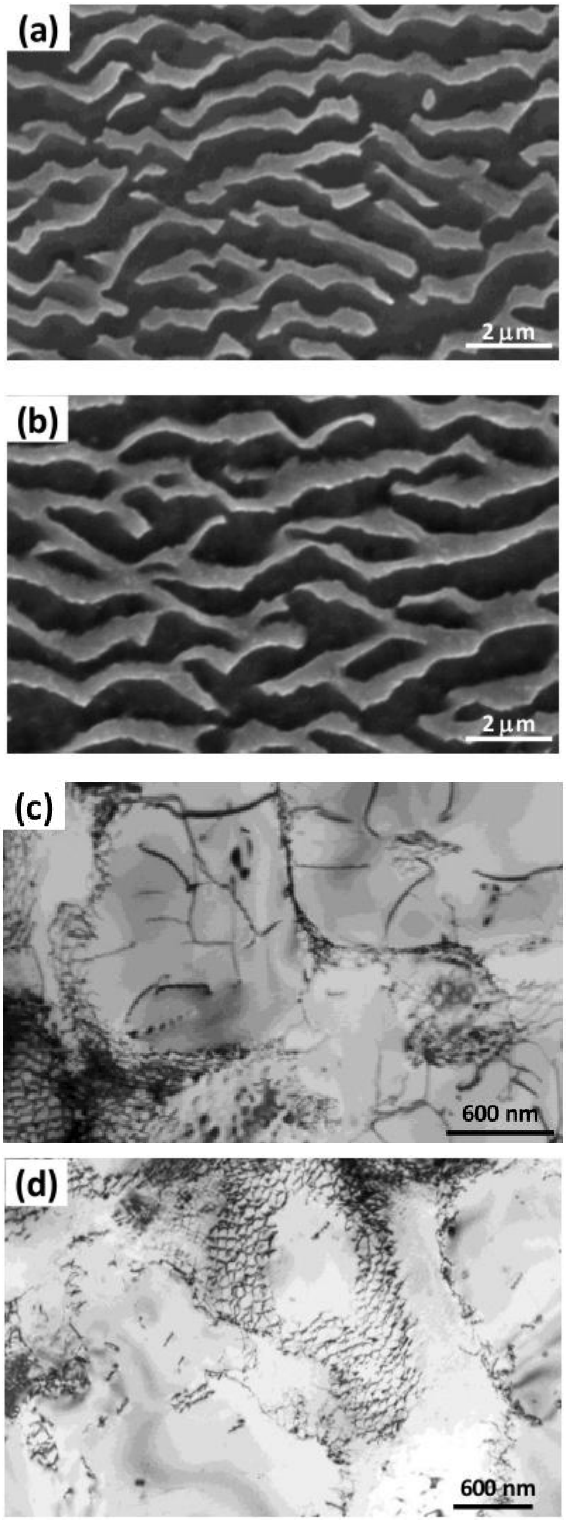

Figure 2. Microstructural evolution after high temperature creep fracture

2.3. Behavior of pore and creep fracture

It can be seen from the fracture morphology of experimental alloy after creep fracture that fracture modes at 1000 °C and 1100 °C are the same as microporous aggregate fracture (figure 3). The creep fracture of is composed of abundant square facets, the orientation of planar edge is <110> direction, and the small circular hole at the center of plane is the origin of the crack. As the temperature rises to 1100°C, the contour of teas plane in the fracture gradually becomes blurry, dimple shape becomes irregular and the number of crack initiation points increases.

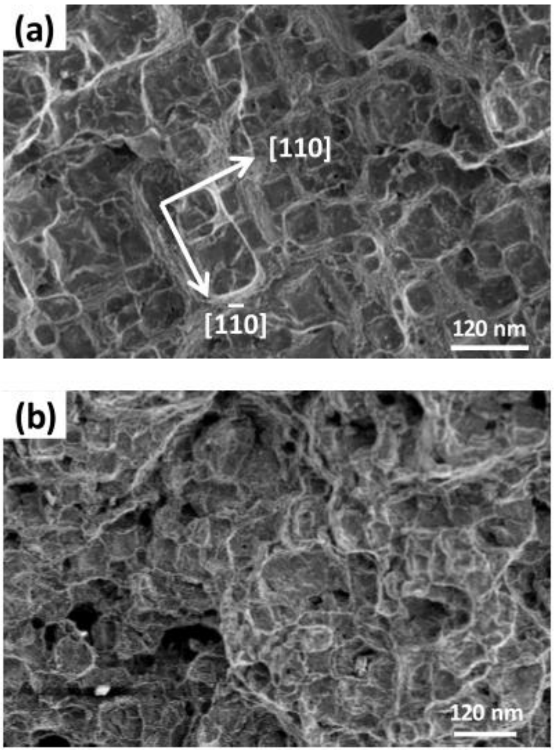

Figure 3. Fracture morphology of alloy after creep fracture

2.4. *Analysis and discussion*

In the temperature and stress ranges of 1000 °C, 160-220 MPa and 1100 °C, 120-150 MPa, the alloys exhibit typical deformation characteristics of the above series of single crystal alloys under high temperature and low stress creep, but it is worth noting that there are also some obvious differences in the creep behavior between the two experimental temperatures. The main manifestations are smaller proportion in the third stage of creep at 1100 °C, faster the deformation rate, and larger density of pores after creep fracture. However, the number of dislocations in the γ′ phase and the creep elongation both are large in the third stage of creep at 1000 °C.

The controlling factor of creep in the initial stage is the slip of the a/2<110> dislocation loop in the {111} plane in the transverse matrix channel perpendicular to the applied stress [001] direction, due to the applied stress has the same direction as the γ/γ′ dual-phase mismatch stress ondislocations. The widening of the transverse matrixchannel caused by the γ′ phaseshaped raft will further promote the movements of the dislocation loop. The generation and operation of dislocations are affected by temperature. The number of dislocation sources at 1100 °C is much higher than 1000 °C, so the initial creep content is significantly higher than that of the latter. The results of initial creep are as follows: a large number of matrix dislocations deposit at the interface of dual-phase, begin to form dislocation networks, γ' phase transforms into a raftmicrostructure, and the creep rate decreases gradually under the influence of the dislocation networks.

As the resistance of matrix dislocation movements increases, the deformation rate of initial creep slows down and creep begins to enter steady state. During the creep steady state, raftmicrostructure completely hindersthe longitudinal matrix channel, making it impossible for the dislocations to continue moving in a way that bypass the γ' phase. An important recovery mechanism for maintaining deformation at this time is that dislocations enter the interior of γ' phase in pairs. As mentioned above, during the creep steady state, dislocations cut raft structure. The superlattice dislocations cutting γ' phase will annihilate with the opposite superlattice dislocations on the other side of raft structure, which is the main recovery mechanism of creep steady state.On the other hand, single dislocation cutting mechanism can not explain the formation and growth of pores during creep. The climbing of depositional dislocations at the γ/γ' dual -phase interface can be regarded as another recovery mechanism. Carry and Strudel[20] et al. firstly proposed that the γ/γ' interface dislocation climbing can be regarded as plastic deformation mechanism. Epishin and Link[21-22] et al. pointed out that after creep enters steady state, the 60° dislocations deposited at the γ/γ' interface can perform non-conservative movements along the direction perpendicular to the applied load, which is mainly dominated by the diffusion process. The non-conservative movements can be regarded as a combination of dislocation slipping and negative climbing, which leads to the alloy undergoing plastic deformation parallel to the applied load direction, and the negative climbing of dislocations causing a large number of vacancies to be discharged These vacancies are diffused to pores through the rapid channels such as the interface between raft and matrix, and low angle boundaries, resulting in the growth of pores. The increase of pore volume fraction after creep can be explained by this deformation mechanism.

In summary, there are two main deformation mechanisms after high temperature creep enters steady state, which are dislocations cutting γ' phase and interface dislocations climbing, respectively. Obviously, the dislocations cutting mechanism requires higher stress level, but the interface dislocations climbing mechanism is more dependent on the creep experiment temperature.

3. conclusions

In this work, a nickel-based single crystal alloy was employed to study the high temperature creep under low applied stress behavior at 1000°C, 160-220 MPa, 1100 °C, and 120-150 MPa. The main conclusions are as follows:

(1)The third stage of creep at 1000 °C lasts longer, deformation rate increases slowly, and the elongation of the alloy is larger. However, the deformation rate of the third stage of creep rapidly increases and fractures in a short time at 1100°C, and the total elongation decreases by about 50% compared with the former;

(2)There are two main deformation mechanisms in the high temperature creep steady state , which are dislocation cutting γ' phase and interface dislocation climbing, respectively. The influence of the two mechanisms on creep deformation varies according to temperature and stress conditions. The former requires larger applied stress to press dislocations cutting γ' phase, while the latter requires higher experimental temperature to promote diffusion;

(3)The main deformation mechanism of 1000°C and 160-220 MPa creep steady state is dislocations cutting γ′ phase. In the post stage of creep steady state, the γ/γ′ dual-phase structures become topologically inverted, and the continuous slipping of superlattice dislocation inside the γ′phase causes the aggravation of alloy deformation and creep entering the third stage;
(4)The main deformation mechanism of 1100 °C and 120-150 MPa creep steady state is the migration of γ/γ′ dual-phase interface dislocations. The dislocations slip and negatively climb perpendicular to the main stress axis, and discharge a large number of vacancies, and vacancies diffusing to pores result in the growth of casting pores and the initiation of new creep pores. The cracking of a large number of pores leads the deformation rate of the alloy to rise rapidly and fracture in the third stage of creep.

References

[1] Reed R C 2006 *M The superalloys: Fundamentals andapplications.*
[2] Tang Y, Huang M, Xiong J, et al 2017 *J. Acta Materialia* **126** 336-345.
[3] Ma S, Lv X, Zhang J, et al 2018 *J. Journa of Alloys and Compounds* **743** 372-376.
[4] Liu W, Liu S, Li J, et al 2014 *J. Materials Research Innovations* **18** 445-449.
[5] Wen Z X, Zhang D, Li S, et al 2017 *J. Journal of Alloys and Compounds* **692** 301-312.
[6] Shu D L, Tian S G, Liang S, et al 2010 *J. Journal of Materials Engineering* **45** 93-100.
[7] Li A N, Tian S G, Liang F S, et al 2010 *J. Journal of Materials Engineering* **1** 210-215.
[8] Wang M G, Tian S G, Yu H C, et al 2009 *J. Journal of Aeronautical Materials* **29** 98-102.
[9] Shollock B, Buffiere J, Curtis R, et al 2017 *J. Scripta Materialia* **36** 1471–1478.
[10] Rae C M F, Reed R C 2007 *J. Acta Materialia* **55** 1067-1081.
[11] Tian S, Ding X, Guo Z, et al 2014 *J. Materials Science and Engineering: A* **594** 7-16.
[12] Wollgramm P, D. Bl, Parsa A B, et al 2016 *J. High Temperature Technology* **33** 346-360.
[13] Huang M, Zhuo L, Xiong J, et al 2015 *J. Philosophical Magazine Letters* **95** 1-8.
[14] Pollock T M, Argon A S 1992 *J. Acta Metallurgica Et Materialia* **40** 1-30.
[15] Hafez h S M, Eggeler G, Raabe D 2013 *J. Acta Materialia* **61** 3709-3723.
[16] Probst-hein M, Dlouhy A, Eggeler G 1999 *J. Acta Materialia* **47** 2497-2510.
[17] Zhao Y S, Liu C G, Guo Y Y, et al 2018 *J. Progress in Natural Science:Materials International* **28** 483-488.
[18] Zhang J X, Wang J C, Harada H, et al 2005 *J. Acta Materialia* **53** 4623-4633.
[19] Huang M, Cheng Z, Xiong J, et al 2014 *J. Acta Materialia* **76** 294-305.
[20] Carry C, Strudel J L 1978 *J. Acta Metallurgica* **25** 767-777.
[21] Epishin A, Link T 2004 *J.Philosophical Magazine* **84** 1979-2000.
[22] Link T, Zabler S, Epishin A, et al 2006 *J. Materials Science & Engineering A* **425** 47-54.